

# Flexible Carbon-Nanofiber Connectors with Anisotropic Adhesion Properties\*\*

Hyunhyub Ko, Zhenxing Zhang, Johnny C. Ho, Kuniharu Takei, Rehan Kapadia, Yu-Lun Chueh, Weizhen Cao, Brett A. Cruden, and Ali Javey\*

The ability of gecko lizards and many insects to climb vertical surfaces relies on the hierarchical micro- and nanofibrillar arrayed features on their feet.<sup>[1–3]</sup> The fibrillar structures provide conformal contact with the opposing surfaces to maximize the van der Waals (vdW) interactions.<sup>[4]</sup> These adhesive systems found in nature have inspired researchers to design synthetic adhesives by using fibrillar arrays of polymers and carbon nanotubes (CNTs), which can universally attach to a variety of surfaces.<sup>[5–10]</sup> In addition to these universal adhesives, the fibrillar arrays have also been utilized to design self-selective connectors to bind morphologically self-similar components together. Specifically, we recently reported self-selective connectors based on inorganic/organic nanowire (NW) arrays, in which the vdW interactions are significantly amplified by the interpenetration of the high-aspect-ratio NW components.<sup>[11–13]</sup> In contrast to gecko adhesives, the unisex NW connectors feature self-selective binding with weak adhesion to non-self-similar surfaces arising from the relatively stiff structure of the hybrid NWs. While the potency of the NW connectors has been shown, previous studies have relied on hard and fragile backing layers, such as silicon substrates used for the growth of the inorganic NWs, which is not practical for

applications requiring lightweight, robust, and bendable backing layers.

Herein, we introduce bendable carbon nanofiber (CNF) connectors with mechanically flexible backing and excellent self-selective adhesion properties. CNFs are similar to multi-walled (MW) CNTs but are distinguished by their stacked graphitic, conelike structures, and are often tapered.<sup>[14]</sup> This structure allows individual CNFs to be free-standing and more effective as interpenetrating connectors than similarly grown CNT forests, which suffer from significant entanglement. The flexible CNF connectors are enabled by the direct transfer of vertical CNF arrays (i.e., CNF forests) grown on silicon substrates to plastic substrates. The vertical geometry of the CNF arrays provides strong shear adhesion strength due to the efficient interpenetration of the CNFs with minimal engagement and disengagement forces. Furthermore, by controlling the tilt angle of the CNF arrays, directional shear adhesion properties are enabled.

Figure 1 illustrates the fabrication procedure for flexible CNF connectors. At first, vertical CNFs with a length  $L = 10\text{--}12\ \mu\text{m}$  and a diameter  $d = 50\text{--}100\ \text{nm}$  were grown on Si/SiO<sub>2</sub> substrates by plasma-enhanced chemical vapor deposition (PECVD), as previously reported elsewhere.<sup>[15]</sup> The surface density of the resulting CNF arrays was  $\approx 5\text{--}6\ \text{CNFs}/\mu\text{m}^2$ . Next, the vertical CNF arrays were transferred onto flexible polymer substrates by using a heat-assisted contact-transfer method.<sup>[16,17]</sup> In this method, CNF arrays grown on silicon substrates were brought into contact with a polycarbonate (PC) film (thickness of  $250\ \mu\text{m}$ ) and thermally annealed at  $190\ ^\circ\text{C}$  for 2 h with an applied normal pressure of  $2\text{--}3\ \text{N cm}^{-2}$ . During this process, CNFs were partially embedded into the PC film softened at a temperature over its glass transition temperature ( $\approx 150\ ^\circ\text{C}$ ). Subsequently, the samples were cooled down and the PC films were peeled off from the surface, during which CNFs are readily transferred to the PC substrate due to their weak mechanical anchoring to the original Si/SiO<sub>2</sub> growth substrates. Finally, a thin layer of parylene-N (thickness of 50, 100, 200 nm) was conformally deposited (see Supporting Information, Figure S1) to enhance the binding ability of CNF connectors. The parylene shell increases the contact area due to the enhanced surface compliance and thus improves the adhesion strength of the connectors.<sup>[11]</sup> Additionally, the parylene shell induces self-selective binding by decreasing the pliability of fibrillar structures, therefore resulting in minimal adhesion to flat surfaces.

[\*] Prof. A. Javey, Dr. H. Ko, Z. Zhang, Dr. J. C. Ho, Dr. K. Takei, R. Kapadia, Dr. Y.-L. Chueh, W. Cao  
Department of Electrical Engineering and Computer Sciences  
University of California at Berkeley  
Berkeley, CA 94720 (USA)  
E-mail: ajavey@eecs.berkeley.edu

Z. Zhang  
Key Laboratory for Magnetism and Magnetic Materials of the  
Ministry of Education  
Lanzhou University  
Gansu 730000 (P.R. China)

Dr. B. A. Cruden  
ELORET Corp., 465 S. Mathilda Ave.  
Sunnyvale, CA 94086 (USA)

[\*\*] The authors thank B. E. Schubert and R. Fearing for insightful discussions and suggestions. This work was supported by DARPA/DSO, NSF Center of Integrated Nanomechanical Systems, and Berkeley Sensor and Actuator Center. Z.Z. acknowledges a fellowship from the China Scholarship Council. The CNF synthesis part of this project was supported by a Laboratory Directed Research and Development grant from Lawrence Berkeley National Laboratory.

Supporting Information is available on the WWW under <http://www.small-journal.com> or from the author.

DOI: 10.1002/sml.200901867

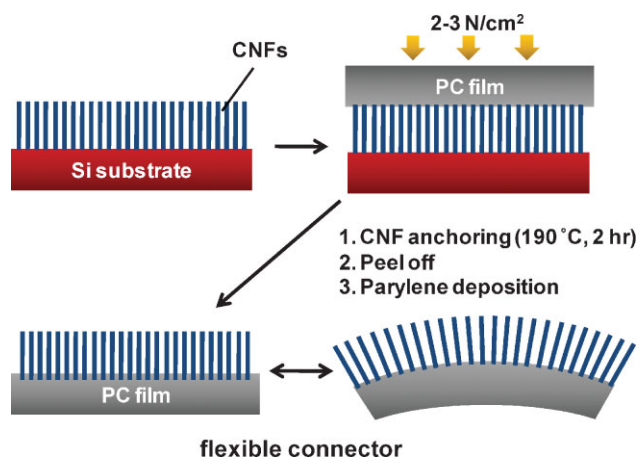


**Figure 1.** Schematic image of the fabrication procedure of flexible CNF connectors. Vertical CNFs grown on silicon substrates are transferred to flexible PC backing layers by heat-assisted (190 °C) contact transfer. To make a conformal contact between CNFs and the PC film, a pressure of 2–3 N cm<sup>-2</sup> was applied between the two substrates.

Figure 2a and b shows scanning electron microscopy (SEM) images of CNF arrays on Si/SiO<sub>2</sub> substrates grown by PECVD. CNFs are straight and uniformly aligned in the vertical direction, which is beneficial for connector applications requiring minimal engagement/disengagement forces. The nanofibers are MWCNT-like, as evident from transmission electron microscopy (TEM) analyses (see Supporting Information, Figure S2). As can be seen in Figure 2c, the

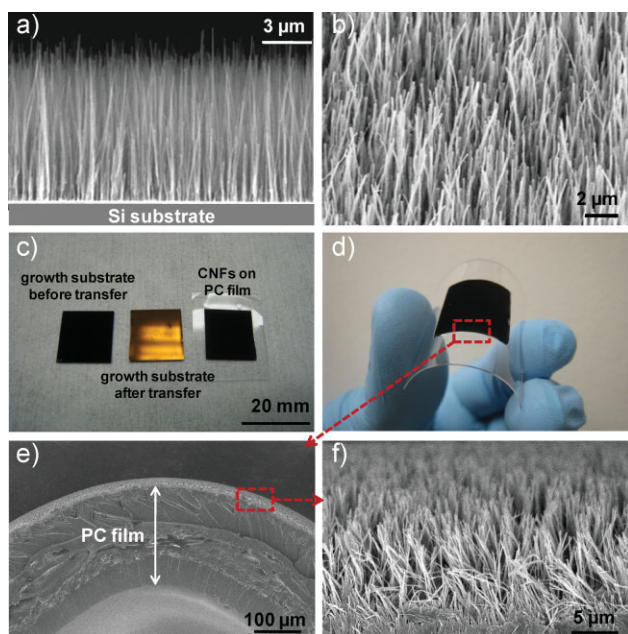


**Figure 2.** a,b) Cross-sectional and tilt-view SEM images of CNF arrays grown on silicon substrates, respectively. c) Optical image of CNF arrays on silicon substrates before (left) and after (middle) the transfer process, and the transferred CNF arrays on a polycarbonate substrate (right). d) Optical image of CNF arrays transferred onto a polycarbonate substrate, showing its flexibility. e,f) Cross-sectional SEM images of CNF arrays transferred to a PC backing layer.

transfer procedure described above provides uniform and complete transfer of vertical CNF arrays from the original growth substrate to the receiver PC substrate over large area (centimeter scale). The transferred CNF arrays on PC backing are bendable, as can be seen in Figure 2d and e. A representative SEM image of the transferred CNF arrays on PC film shows that CNFs maintain their vertical geometry after the transfer process, without bundling or aggregation (Figure 2f). The exposed length of the transferred CNFs is 6–8 μm with an embedded length of ≈4 μm (Figure 2f). This partial embedment of CNFs provides mechanical robustness and strong adhesion and anchoring of CNFs to the PC substrates, which are needed for robust connector applications.

To characterize the binding capability of CNF connectors, we performed macroscopic shear and normal adhesion tests. For the macroscopic adhesion tests, a normal preload pressure of ≈4 N cm<sup>-2</sup> was first applied to engage the morphologically self-similar (“unisex”) mates of the CNF connectors (area ≈0.25 cm<sup>2</sup>). The preload force was then removed to measure the pure shear or normal adhesion strengths (Figure 3a). The shear adhesion strength of CNF connectors strongly depends on the parylene shell thickness (*t<sub>p</sub>*), as shown in Figure 3b. Notably, a shear adhesion strength of ≈25 N cm<sup>-2</sup> is obtained

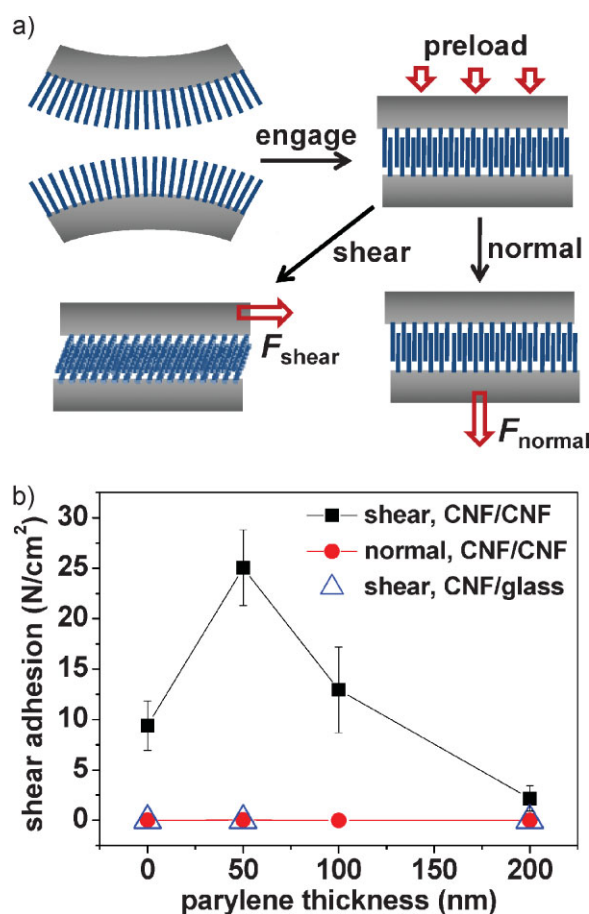


**Figure 3.** a) Schematic images of the shear and normal adhesion measurements of flexible CNF connectors. b) Shear and normal adhesion strengths of flexible CNF connectors as a function of the parylene shell thickness. The preload pressure used to engage the CNF connectors was ≈4 N cm<sup>-2</sup>.

for  $t_p = 50$  nm, which is significantly higher than that of the pristine CNFs ( $\approx 9$  N cm $^{-2}$ ). However, the shear adhesion strength of the connectors decreases with further increase of parylene shell thickness (Figure 3b). The modulation of shear adhesion with  $t_p$  can be explained by two competing factors, that is, contact area and filling factor, similar to our previous reports on hybrid NW structures.<sup>[11,12]</sup> Briefly, for thin parylene thicknesses ( $t_p = 50$  nm), the higher surface compliance of the parylene shell on the hard CNFs enables conformal contact with increased contact area between the interpenetrating CNFs. Beyond a critical thickness ( $t_p \approx 100$  nm), however, the filling factor becomes too large for efficient interpenetration of the engaged CNFs for a given preload pressure.

In contrast to the gecko adhesives, which universally adhere to most surfaces, the CNF connectors show self-selective binding with minimal adhesion to flat surfaces, such as a clean glass surface (Figure 3b) mainly due to the low bendability of the relatively short (6–8  $\mu$ m) and large-diameter (50–100 nm) CNFs used in this work. Previous studies utilizing vertical CNTs for universal gecko adhesives were based on long ( $L = 200$ – $1000$   $\mu$ m) and small-diameter (1–20 nm) nanotubes, which are more bendable and have significant entanglement, both of which enhance side contact with flat surfaces and therefore are not self-selective.<sup>[6,7,9,18,19]</sup>

A unique feature of the CNF connectors is their high shear-to-normal-adhesion ratio, ideal for applications in which strong shear adhesion with low detachment forces are necessary.<sup>[20,21]</sup> As can be seen in Figure 3b, CNF connectors show almost no measurable adhesion strength ( $< 0.05$  N cm $^{-2}$ ) in the normal direction, regardless of the parylene shell thickness. Specifically, the shear-to-normal-adhesion ratios over 300 are obtained for all parylene thicknesses ( $t_p = 0, 50, 100, 200$  nm) tested in this study. This shear-to-normal-adhesion ratio is  $\approx 11\times$  higher than our previous connectors (shear-to-normal-adhesion ratio of  $\approx 27$ ) based on randomly oriented NW arrays. The low normal adhesion strength of CNF connectors is attributed to the vertical geometry and low bendability of the CNF arrays utilized in this study, which minimizes the mechanical entanglement. Although the overall adhesion is likely to be due to a complex combination of various forces, our previous work on nanowire connectors with parylene surface have demonstrated the dominant role of vdW interactions, which can be enhanced with an increase of the contact area.<sup>[11,13]</sup> When the engaged connectors are under a shear force, the vertical CNFs are aligned in the shear direction and thus provide a higher probability of side contact between the interpenetrating CNFs. However, the contact area between the vertical CNFs is small without a shear force, resulting in low normal adhesion strengths.

The shear adhesion strength of CNF connectors is affected by the applied preload pressure to engage the connectors. As can be seen in Figure 4a, the maximum shear strength of CNF connectors increases with the applied normal preload. Specifically, the shear adhesion of CNF connectors increases from 9 to 78 N cm $^{-2}$  when the preload force increases from 0.9 to 93 N cm $^{-2}$ . This shear adhesion strength of 78 N cm $^{-2}$  obtained for a connector with flexible backing is well above the shear-adhesion strengths of most common connectors such as Velcro (5–15 N cm $^{-2}$ )<sup>[22]</sup> and comparable to those achievable for CNT

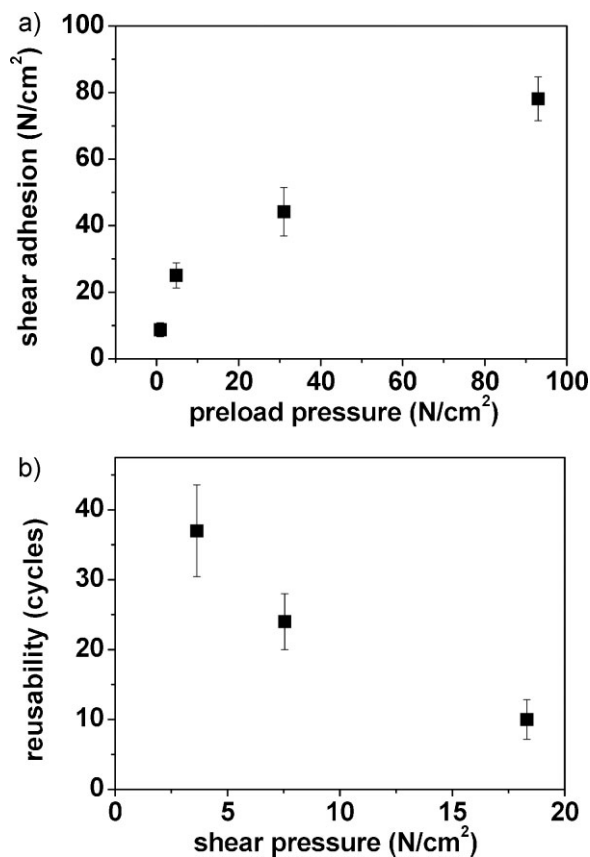


**Figure 4.** a) Shear adhesion strength of CNF connectors as a function of the applied normal preload pressure. b) Reusability of CNF connectors as a function of shear pressure with a preload of  $\approx 3.6$  N cm $^{-2}$ . The parylene shell thickness is 50 nm.

gecko adhesives with hard backing (30–100 N cm $^{-2}$ ).<sup>[6,9,19]</sup> The increase of shear adhesion with preload can be explained by the increase of interpenetration depth and thus enhanced contact area between the engaged CNFs. The incremental increase in shear adhesion with preload reduces at large preload pressures ( $> 4.8$  N cm $^{-2}$ ) as the interpenetration depth approaches its maximum value.

Reusability is an important characterization metric for practical connector applications. Reusability tests were performed by attaching/detaching the connectors for multiple cycles until the connectors failed to maintain the applied shear pressure. Here, we tested reusability of CNF connectors at a fixed shear pressure, lower than the maximum shear strength, to examine the number of cycles that the connectors can successfully operate within their operational limit. CNF connectors show a reusability of  $\approx 37$  times for a preload and a shear pressure of  $\approx 3.6$  N cm $^{-2}$  (Figure 4b). This reusability is a significant improvement over the previous CNT adhesives on hard backing, which could operate only a few cycles.<sup>[18]</sup> It is noteworthy that the CNF connectors maintained good reusability even at a high shear force (e.g.,  $\approx 10$  times at 18 N cm $^{-2}$ ). The high reusability of CNF connectors reported here arises from the partial embedment of the CNF arrays in the PC film, therefore providing a mechanical support at the base, which is often the failure site.

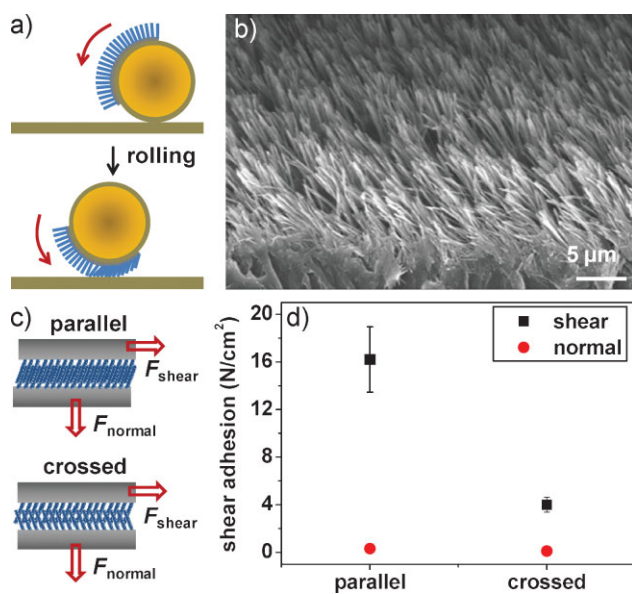


**Figure 5.** a) Schematic image of the fabrication procedure for tilted CNF connectors. The CNF arrays on a PC backing were mounted on cylindrical tubes and rolled on a planar PDMS substrate to enable uniform tilting of the CNF arrays. b) Angled-view and top-view SEM images of tilted CNF arrays on a PC substrate. c) Schematic image of the shear and normal adhesion tests for the parallel and crossed engagements of the tilted CNF arrays. d) Shear and normal adhesion strengths of the tilted CNF connectors.

To further demonstrate the versatility of the CNF connectors, tilted CNF arrays were fabricated to provide anisotropic shear adhesion properties. Previously, synthetic gecko adhesives have been shown to provide directional adhesion capabilities when they are uniformly tilted due to the strong adhesion along the tilt direction of the fibrillar arrays as compared to that of the opposite direction.<sup>[23–26]</sup> To fabricate tilted CNF connectors, CNF arrays on a PC backing (15 × 12-mm area) were mounted on a polydimethylsiloxane (PDMS) film (≈1-mm thick) and wrapped around a cylindrical tube (2.8-cm diameter). Then, the cylindrical tube was brought into contact with a flat PDMS substrate (≈2-mm thick) and rolled with a speed of ≈2 mm s<sup>-1</sup> and a normal force of ≈20 N. During this rolling process, CNFs on the cylindrical tube were tilted by the induced shear force. As can be seen from the SEM images in Figure 5b, the CNF arrays on PC film were uniformly tilted with an angle of ≈30°. After the rolling process, a parylene shell (≈50-nm thick) was deposited to firmly mold the orientation of the titled CNF arrays.

The tilted CNF connectors show strong directional adhesion properties. When the tilted CNFs on the top and bottom mates are in parallel (i.e., parallel configuration, Figure 5c), the connectors showed a shear adhesion strength of ≈16 N cm<sup>-2</sup> at a preload of ≈4 N cm<sup>-2</sup> (Figure 5d). However, a shear adhesion strength of only ≈4 N cm<sup>-2</sup> (Figure 5d) was obtained when the tilted CNFs of the two mates are engaged in an antiparallel orientation (i.e., crossed configuration, Figure 5c). This strong anisotropic adhesion behavior is attributed to the increased contact area for parallel engagement as compared to the crossed engagement, partly due to the

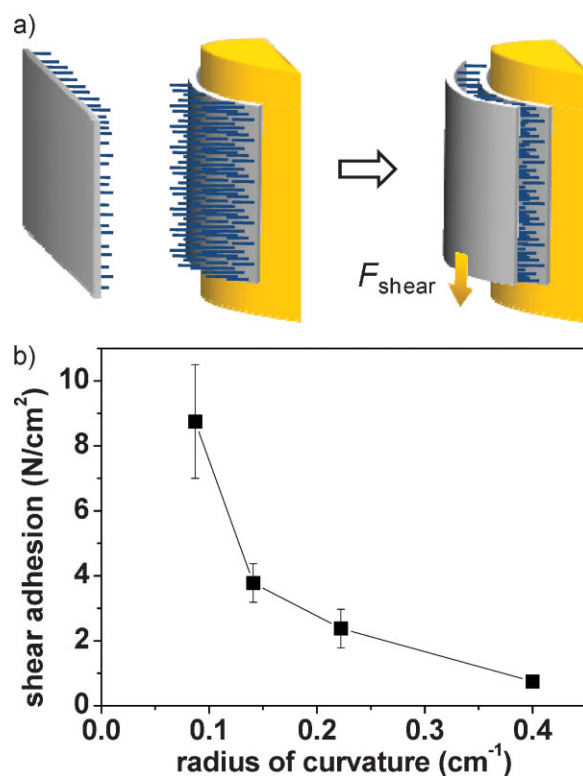


**Figure 6.** a) Schematic image of the shear adhesion measurements of flexible CNF connectors attached on a curved surface. b) Shear adhesion strength of flexible CNF connectors as a function of the radius of curvature.

higher interpenetration depth for a given preload. It is worthwhile to note that the minimal normal adhesion was observed for tilted CNF connectors (≈0 N cm<sup>-2</sup>) for both directions of engagement, demonstrating anisotropic adhesion properties in multiple orientations.

A unique feature of the CNF connectors presented here, different from our previous nanoconnectors, lies in their mechanical bendability. To examine the effect of bending on the adhesion performance of the connectors, we tested the shear adhesion strength as a function of the radius of curvature (Figure 6). As can be seen in Figure 6b, the performance of CNF connectors strongly depends on the radius of curvature with a decrease in the adhesion strength with the bending curvature. This behavior is attributed to the elastic recovery stress of the bent support substrate (i.e., polycarbonate) used in this work. Since the substrate recovery bending stress increases with the increase of bending curvature, the CNF connectors more readily detach as they are bent to a larger radius. In the future, the performance of CNF connectors can be improved by optimizing the modulus and thickness of the polymeric support substrate.

In conclusion, a simple strategy for the fabrication of versatile CNF connectors with mechanically flexible backing is demonstrated. The connectors show excellent anisotropic and self-selective binding with strong shear but weak normal adhesion strength. In addition, we further control the anisotropic adhesion properties within the shear regime by uniformly tilting the vertical CNF arrays. The CNF connectors

introduced in this study may have important implications for applications requiring self-selective connectivity of the components with lightweight, robust, and bendable backing layers.

### Experimental Section

**CNF growth:** Vertical CNFs (length  $L \approx 10\text{--}12\ \mu\text{m}$ , diameter  $d \approx 50\text{--}100\ \text{nm}$ ) were grown on Si/50 nm SiO<sub>2</sub>/200 nm Cu/30 nm Ti/30 nm Ni substrates by PECVD. CNFs were grown at 900 °C, 5 Torr, plasma power of 210W, and C<sub>2</sub>H<sub>2</sub>/NH<sub>3</sub> gas flow of 22.5/80 sccm with a typical growth rate of 0.15  $\mu\text{m min}^{-1}$ .

**Shear adhesion test:** The shear adhesion strengths of flexible CNF connectors with different parylene thickness were tested by first applying a normal preload force to the NW connectors ( $\approx 0.5 \times 0.5\ \text{cm}^2$ ) followed by applying a shear force, and finally removing the preload to measure the pure shear force strength. Shear adhesion tests for each reported condition were done for 3–4 samples and the average values used. Parylene-N was deposited on the CNF arrays on PC substrates by using a PDS 2010 Labcoter 2 (Specialty Coating Systems) deposition system. For the bending adhesion tests, the flexible CNF connectors were attached to curved surfaces with different radii of curvature and the shear adhesion strengths were measured.

### Keywords:

anisotropy · carbon nanofibers · directional adhesion · flexible materials

- [1] E. Arzt, S. Gorb, R. Spolenak, *Proc. Natl. Acad. Sci. USA* **2007**, *100*, 10603.  
 [2] A. M. Peattie, R. J. Full, *Proc. Natl. Acad. Sci. USA* **2007**, *104*, 18595.  
 [3] W. Federle, *J. Exp. Biol.* **2006**, *209*, 2611.  
 [4] K. Autumn, M. Sitti, A. Peattie, W. Hansen, S. Sponberg, Y. A. Liang, T. Kenny, R. Fearing, J. Israelachvili, R. J. Full, *Proc. Natl. Acad. Sci. USA* **2002**, *99*, 12252.  
 [5] K. Autumn, Y. A. Liang, S. T. Hsieh, W. Zesch, W.-P. Chan, W. T. Kenny, R. Fearing, R. J. Full, *Nature* **2000**, *405*, 681.  
 [6] L. Qu, L. Dai, M. Stone, Z. Xia, Z. L. Wang, *Science* **2008**, *322*, 238.  
 [7] L. Ge, S. Sethi, L. Ci, P. M. Ajayan, A. Dhinojwala, *Proc. Natl. Acad. Sci. USA* **2007**, *104*, 10792.  
 [8] M. Murphy, B. Aksak, M. Sitti, *J. Adhesion Sci. Technol.* **2007**, *21*, 1281.  
 [9] L. Qu, L. Dai, *Adv. Mater.* **2007**, *19*, 3844.  
 [10] G. Huber, H. Mantz, R. Spolenak, K. Mecke, K. Jacobs, S. N. Gorb, E. Arzt, *Proc. Natl. Acad. Sci. USA* **2005**, *102*, 16293.  
 [11] H. Ko, J. Lee, B. E. Schubert, Y.-L. Chueh, P. W. Leu, R. S. Fearing, A. Javey, *Nano Lett.* **2009**, *9*, 2054.  
 [12] R. Kapadia, H. Ko, Y.-L. Chueh, J. C. Ho, T. Takahashi, Z. Zhang, A. Javey, *Appl. Phys. Lett.* **2009**, *94*, 263110.  
 [13] H. Ko, Z. Zhang, Y.-L. Chueh, J. C. Ho, J. Lee, R. S. Fearing, A. Javey, *Adv. Funct. Mater.*, **2009**, *19*, 3098.  
 [14] L. Delzeit, I. McAninch, B. A. Cruden, D. Hash, B. Chen, J. Han, M. Meyyappan, *J. App. Phys.* **2002**, *91*, 6027.  
 [15] B. A. Cruden, A. M. Cassell, Q. Ye, M. Meyyappan, *J. Appl. Phys.* **2003**, *94*, 4070.  
 [16] T. Y. Tsai, C. Y. Lee, N. H. Tai, W. H. Tuan, *Appl. Phys. Lett.* **2009**, *95*, 013107.  
 [17] E. Sunden, K. Moon, C. P. Wong, W. P. King, S. Graham, *J. Vac. Sci. Technol. B* **2006**, *24*, 1947.  
 [18] Y. Zhao, T. Tong, L. Delzeit, A. Kashani, M. Meyyappan, A. Majumdar, *J. Vac. Sci. Technol. B* **2006**, *24*, 331.  
 [19] Y. Maeno, Y. Nakayama, *Appl. Phys. Lett.* **2009**, *94*, 012103.  
 [20] K. Autumn, *MRS Bull.* **2007**, *32*, 473.  
 [21] K. Autumn, A. Dittmore, D. Santos, M. Spenko, M. Cutkosky, *J. Exp. Bio.* **2006**, *209*, 3569.  
 [22] www.torstamp.com/Brochures/BR-122.pdf  
 [23] H. E. Jeong, J.-K. Lee, H. N. Kim, S. H. Moon, K. Y. Suh, *Proc. Natl. Acad. Sci. USA* **2009**, *106*, 5639.  
 [24] M. Murphy, B. Aksak, M. Sitti, *Small* **2009**, *5*, 170.  
 [25] J. Lee, R. S. Fearing, K. Komvopoulos, *Appl. Phys. Lett.* **2008**, *93*, 191910.  
 [26] T.-I. Kim, H. E. Jeong, K. Y. Suh, H. H. Lee, *Adv. Mater.* **2009**, *21*, 1.

Received: October 2, 2009  
Published online: